L. W. Anderson, and W. Haeberli, Phys. Rev. 174, 201 (1968).
[13]J. Perel and H. L. Daley, Bull. Am. Phys. Soc. 13, 614 (1968).
[14]J. Perel and H. L. Daley, Bull. Am. Phys. Soc. 14, 259 (1969).
[15]H. L. Daley and J. Perel, AIAA J. 7, 733 (1969).
[16]H. L. Daley and J. Perel, Bull. Am. Phys. Soc. 14, 1179 (1969).
[17]G. F. Drukarev, in Ref. 6, p. 10.
[18]D. V. Chkuaseli, A. I. Guldamashvilli, and V. D. Nikoleyishvilli, Bull. Acad. Sci. USSR 27, 976 (1963).
[19]L. L. Marino, Phys. Rev. 152, 46 (1966).
[20]L. L. Marino, *Atomic Collision Processes* (North-Holland, Amsterdam, 1964), p. 807.
[21]J. Perel and H. L. Daley, Bull. Am. Phys. Soc. 14, 1179 (1969).
[22]J. Perel and H. L. Daley, Bull. Am. Phys. Soc. 13, 1656 (1968).
[23]J. Perel and H. L. Daley, Ref. 7, p. 1055.
[24]L. I. Pivovar, L. I. Nikolaichuk, and A. N. Grigor Grigor'ev, Zh. Eksperim. i Teor. Fiz. 57, 432 (1969) [Sov. Phys. JETP 30, 236 (1970)].
[25]H. L. Daley and J. Perel (unpublished).
[26]H. R. Kaufman and P. D. Reader, in *AIAA Progress in Astronautics and Aeronautics: Electrostatic Propulsion*, edited by D. B. Langmuir, E. Stuhlinger, and J. M. Sellen, Jr. (Academic, New York, 1961), Vol. 5, p. 3.
[27]J. Perel, J. Electrochem. Soc. 115, 34C (1968).
[28]W. Bleakney, Phys. Rev. 35, 139 (1930).
[29]W. Ramsey (private communication).
[30]H. L. Daley, A. Y. Yahiku, and J. Perel, J. Chem. Phys. 52, 3577 (1970).
[31]J. Perel, Rev. Sci. Instr. 39, 394 (1968).
[32]J. Perel, H. L. Daley, and F. J. Smith, Phys. Rev. A 1, 1626 (1970).
[33]Notation taken from C. Candler, *Atomic Spectra* (Van Nostrand, Princeton, N. J., 1964).
[34]G. Herzberg, *Spectra of Diatomic Molecules* (Van Nostrand, Princeton, N. J., 1959), p. 267.

PHYSICAL REVIEW A VOLUME 4, NUMBER 1 JULY 1971

Low-Energy Elastic and Fine-Structure Excitation Scattering of Ground-State C^+ Ions by Hydrogen Atoms†

Jon C. Weisheit* and Neal F. Lane‡
Department of Physics, Rice University, Houston, Texas 77001
(Received 18 January 1971)

Cross sections are computed for the elastic and fine-structure excitation scattering of singly ionized carbon atoms by low-energy (less than 0.1 eV) hydrogen atoms. A close-coupling formulation is employed and the scattering equations are solved in a coupled-angular-momentum representation. The correct energy defect between the $C^+(^2P)$ fine-structure levels is included. For the first time, both spin-change and long-range electrostatic coupling terms are explicitly included in the scattering equations. The calculated C^+-H excitation cross section varies from 4.87×10^{-15} cm^2 at 0.01 eV to 2.86×10^{-15} cm^2 at 0.085 eV, and the maximum of almost 5.60×10^{-15} cm^2 occurs near 0.015 eV. The spin-change coupling, described herein, is found to be much more important than the long-range electrostatic coupling at all energies considered.

I. INTRODUCTION

Recent surveys[1,2] have emphasized the importance of heavy-particle collisions in astrophysics. In particular, calculations of the fine-structure excitation cross sections of $C(^3P)$, $C^+(^2P)$, $O(^3P)$, and $Si^+(^2P)$ atoms in collision with slow $H(^2S)$ atoms have indicated that in the interstellar medium these reactions have large rate coefficients.[3-8] Such collisional excitations and the subsequent forbidden radiative decays provide a significant cooling mechanism for interstellar gas.

Each of the theoretical investigations cited above has included the simplifying approximation that the excitation processes are elastic, i.e., that the energy differences between fine-structure levels are small in comparison with the center-of-mass kinetic energy of the colliding atoms and consequently may be neglected. Temperatures corresponding to the excitation energies ($\Delta T = \Delta E/k_B$, where k_B is the Boltzmann constant) of the C, C^+, O, Si, and Si^+ ground-state fine-structure levels range from 23 to 411 °K. It is evident that in interstellar space, where the temperature is typically 125 °K,[1] these fine-structure excitation collisions are highly inelastic events and thus the approximation of elastic scattering may be quite inappropriate. Furthermore, in all previous work the assumption has been made that the scattering is dominated entirely by the spin-change process[3,5,7,8] or by the orientation-dependent electrostatic interaction.[4,6] Up to the present time there have been no

calculations employing formulations general enough to determine the relative importance of these two "interactions."

In this paper the scattering of singly ionized carbon atoms by slow hydrogen atoms is considered in detail. For the first time, both the electrostatic interaction and the spin-change interaction are included in the same calculation. A close-coupling formalism is used to compute the $C^+(^2P)$-$H(^2S)$ elastic and fine-structure excitation cross sections. Inclusion of the spin-change interaction in a close-coupling treatment requires detailed knowledge of the relevant molecular potential curves (see Sec. II). The C^+-H collision was specifically chosen for our investigation because of the availability of these curves.[9,10] The scattering equations are derived and solved numerically in a coupled-angular-momentum representation and the fine-structure splitting of the $C^+(^2P)$ state is correctly accounted for.

Our results indicate that the spin-change interaction is the more important one, at least at energies considered here ($E < 0.086$ eV or $T < 1000$ °K). Consequently, the C^+-H spin-change excitation cross sections computed by Smith[7] and by Wofsy *et al.*[8] are in better agreement with our calculations than those computed by Callaway and Dugan,[6] who included only the electrostatic interaction.

The remainder of the paper is organized as follows. In Sec. II the close-coupling formalism is briefly reviewed and then applied to the C^+-H scattering problem. The coupling matrix elements for the spin-change and electrostatic interactions are then derived and simplified by Racah algebra techniques. The numerical methods used to integrate the coupled equations are described in Sec. III. At this point the CH^+ electronic curves are also introduced. In Sec. IV the $C^+(^2P)$-$H(^2S)$ elastic and fine-structure excitation cross sections are presented and discussed. The reaction rate coefficient for the excitation process is also given. Finally, a detailed derivation of the spin-change coupling matrix elements is given in the Appendix.

II. THEORY

A complete discussion of the close-coupling formalism and its application to atom-atom collision problems has been given elsewhere (see, for example, Mott and Massey,[11] Chaps. 12–13); we include here only the essential points. Atomic units are used throughout.

Consider the collision of two atoms A and B. Let H_A and H_B, $\psi_A(\alpha)$ and $\psi_B(\beta)$, and $E_A(\alpha)$ and $E_B(\beta)$ be the respective Hamiltonians, antisymmetrized eigenfunctions, and eigenvalues for the isolated atoms, with α and β being appropriate sets of quantum numbers. Then we have

$$H_A\psi_A(\alpha) = E_A(\alpha)\psi_A(\alpha) , \tag{1}$$

with a similar equation holding for atom B.

The Schrödinger equation satisfied by the wave function Ψ describing the relative and internal motions of A and B is

$$[-(1/2\mu)\nabla_R^2 + H_A + H_B + V]\Psi = E\Psi , \tag{2}$$

where μ is the reduced mass of the colliding atoms, $\vec{R}$ is the separation of their nuclear centers of mass, V is the electrostatic atom-atom interaction potential energy, and E is the total relative energy. Since $\psi_A(\alpha)$ and $\psi_B(\beta)$ are members of complete sets of eigenfunctions, Ψ may be expanded in terms of the antisymmetrized product functions $\psi_A(\alpha)\psi_B(\beta)$. However, a simple antisymmetrized product representation is not the most convenient one. The total Hamiltonian of the scattering system is invariant with respect to spatial rotations and so the total angular momentum $\vec{J}$ commutes with the Hamiltonian of Eq. (2), and in fact commutes with each term of this Hamiltonian. As a result, the matrix of the interaction potential V is diagonal in a coupled (JM) representation.

We choose to couple first $\vec{j}_\alpha$, the total angular momentum of A in state α, and $\vec{l}$, the angular momentum of relative motion, to yield $\vec{\mathcal{J}}$; and then couple $\vec{\mathcal{J}}$ and $\vec{j}_\beta$, the total angular momentum of B in state β, to yield $\vec{J}$. Thus, we have

$$(\vec{j}_\alpha + \vec{l}) + \vec{j}_\beta = \vec{\mathcal{J}} + \vec{j}_\beta = \vec{J} . \tag{3}$$

In this coupled representation the total wave function Ψ may be expanded in terms of coupled angular basis functions

$$\Psi^{JM} = \sum_{j_\alpha j_\beta l \mathcal{J}} [(1/R) f^J_{j_\alpha j_\beta l \mathcal{J}}(R) \Gamma^{JM}_{j_\alpha j_\beta l \mathcal{J}}] , \tag{4}$$

where

$$\Gamma^{JM}_{j_\alpha j_\beta l \mathcal{J}} = \sum_{\mathfrak{M} m_\beta} (\mathcal{J}\mathfrak{M}\, j_\beta m_\beta | JM) \psi_B(j_\beta m_\beta) \mathcal{Y}^{\mathcal{J}\mathfrak{M}}_{j_\alpha l} , \tag{5}$$

$$\mathcal{Y}^{\mathcal{J}\mathfrak{M}}_{j_\alpha l} = \sum_{m_\alpha m} (j_\alpha m_\alpha l m_l | \mathcal{J}\mathfrak{M}) \psi_A(j_\alpha m_\alpha) Y_{l m_l}(\hat{R}) , \tag{6}$$

and where $(j_1 m_1 j_2 m_2 | j_3 m_3)$ is a Clebsch-Gordan coefficient, $Y_{lm}(\hat{R})$ is a spherical harmonic, and $\hat{R}$ is the orientation of the internuclear axis $\vec{R}$. The incident-beam direction is chosen as the polar axis.

The radial function $f^J_{j_\alpha j_\beta l \mathcal{J}}(R)$ describes the relative motion of atoms A and B. For brevity we shall denote the set of quantum numbers $(j_\alpha j_\beta l \mathcal{J})$ by the index γ, and then write the particular radial functions appropriate to the initial condition γ_0 as $f^J_{\gamma\gamma_0}(R)$. The coupled equations which the $f^J_{\gamma\gamma_0}$ satisfy are obtained from the Schrödinger equation (2) using familiar procedures. These equations are

$$\left[\frac{d^2}{dR^2} - \frac{l(l+1)}{R^2} + k_\gamma^2\right] f^J_{\gamma\gamma_0}(R)$$

$$= 2\mu \sum_{\gamma'} V^J_{\gamma\gamma'}(R) f^J_{\gamma'\gamma_0}(R) \quad , \quad (7)$$

where

$$k_\gamma^2 = 2\mu[E - E_A(\alpha) - E_B(\beta)] \quad , \quad (8)$$

and where the coupling matrix element is

$$V^J_{\gamma\gamma'}(R) = \int dR^{-1} [\Gamma^{*JM}_\gamma V \Gamma^{JM}_{\gamma'}] \quad , \quad (9)$$

the integration being performed with respect to all coordinates but R. The fact that $V^J_{\gamma\gamma'}$ is independent of M simply reflects the rotational invariance of V.

The close-coupling approximation consists of restricting the infinite summation in (7) to a certain few atomic states $\psi_A(\alpha)$ and $\psi_B(\beta)$. We now turn to the specific problem of low-energy scattering of $C^+(^2P)$ by $H(^2S)$. The following discussion of the coupling matrix elements will make clear which atomic states should be included in our calculations.

The dominant force between two atoms distant enough that their wave functions do not overlap arises from the electrostatic interaction. It is well known that, if either of the two atoms is neutral and possesses a spherical charge distribution (S state), the long-range electrostatic interaction energy vanishes to first order.[12] Consequently, if we include only the ^2S ground state of hydrogen in the equations (7) and neglect exchange terms, all of the long-range electrostatic coupling matrix elements are identically zero.

Now at energies of interest here all of the excited states of hydrogen are inaccessible during the collision. It can be shown, however, that including all of these states in the coupled equations provides an effective interaction potential v for the scattering of the carbon ion.[13,14] This effective potential is due to the virtual excitation of the ground-state hydrogen atom by the carbon ion and, in fact, is well represented by the second-order energy correction for the hydrogen atom perturbed by the ion. A straightforward perturbation calculation yields[15]

$$v(\vec{R},\vec{r}) = -\frac{\alpha_2}{2R^4}\left(1 - 4\frac{r}{R} P_1(\hat{r}\cdot\hat{R}) + \frac{r^2}{R^2}[2 - 4P_2(\hat{r}\cdot\hat{R})]\right)$$

$$- \frac{\alpha_4}{2R^6} + O(R^{-7}) \quad , \quad (10)$$

where α_{2L} is the 2^L-pole polarizability of hydrogen, $\vec{r}$ is the coordinate of the $C^+(2p)$ electron, and $P_\lambda(\hat{r}\cdot\hat{R})$ is the λth-order Legendre polynomial. Except for the additional term $-\alpha_4/2R^6$ the above expression is identical to that used by Callaway and Dugan.[6]

It should be emphasized that in the coupling matrix elements the second-order interaction energy $v(\vec{R},\vec{r})$ replaces the vanishing first-order term $\langle\psi_H(1s)|V|\psi_H(1s)\rangle$.

Writing v in the more general form,

$$v(\vec{R},\vec{r}) = \sum_\lambda v_\lambda(R,r) P_\lambda(\hat{r}\cdot\hat{R}) \quad , \quad (11)$$

coupling matrix elements may be evaluated by the methods of Racah algebra with the result[16]

$$V^J_{\gamma\gamma'}(R) = \sum_{\mathfrak{M}\mathfrak{M}'\sigma} (\mathcal{J}\mathfrak{M}\tfrac{1}{2}\sigma|JM)(\mathcal{J}'\mathfrak{M}'\tfrac{1}{2}\sigma|JM)\langle \mathcal{Y}^{\mathcal{J}\mathfrak{M}}_{jl}|v|\mathcal{Y}^{\mathcal{J}'\mathfrak{M}'}_{j'l'}\rangle$$

$$= 3\delta(\mathcal{J},\mathcal{J}')\delta(\mathfrak{M},\mathfrak{M}')[(2l+1)(2l'+1)(2j+1)(2j'+1)]^{1/2} \sum_\lambda (-)^{\mathcal{J}-1/2-\lambda} v_\lambda(R) \begin{pmatrix} 1 & \lambda & 1 \\ 0 & 0 & 0 \end{pmatrix} \begin{pmatrix} l & \lambda & l' \\ 0 & 0 & 0 \end{pmatrix} \begin{Bmatrix} j & j' & \lambda \\ 1 & 1 & \frac{1}{2} \end{Bmatrix} \begin{Bmatrix} j & j' & \lambda \\ l' & l & \mathcal{J} \end{Bmatrix}$$

$$= \sum_\lambda v_\lambda(R) q_\lambda(jl\mathcal{J}, j'l'\mathcal{J}') \quad , \quad (12)$$

say, where

$$\begin{pmatrix} j_1 & j_2 & j_3 \\ m_1 & m_2 & m_3 \end{pmatrix} \text{ and } \begin{Bmatrix} j_1 & j_2 & j_3 \\ j_4 & j_5 & j_6 \end{Bmatrix}$$

are 3-j and 6-j symbols; the index j now represents the total angular momentum of the carbon ion, and the v_λ have been averaged with respect to the $C^+(2p)$ orbital.

The utility of our coupling scheme Eq. (3) is apparent in Eq. (12). The quantities q_λ are diagonal in $\mathcal{J}$ and $\mathfrak{M}$, independent of $\mathfrak{M}$, and independent of J. Also, we see that here only even values of λ contribute nonvanishing coupling terms.

The coupling matrix elements $V^J_{\gamma\gamma'}$ must be modified at small internuclear separations to allow for the possibility of electron exchange. To do this we adapt the spin-change mechanism described by Dalgarno[17] and Dalgarno and Rudge[18] to the close-coupling formalism. Briefly, in a spin-change collision the internal angular momenta of colliding systems may change because of the possible exchange of electrons with different spin orientations. In the formulation of Dalgarno, where spin-orbit

and spin-spin interactions in the molecule are omitted, the scattering is elastic in the molecular representation where Λ, S, and M_S are the total orbital angular momentum (projected onto the body axis $\vec{R}$), total spin angular momentum, and its projection (onto $\vec{R}$) of the CH^+ molecule in the state $\chi(\Lambda SM_S)$.

If the energy defect between atomic fine-structure levels is neglected, the elastic scattering amplitude $f(\Lambda SM_S, \Lambda SM_S; \hat{R})$ is related to the amplitude $f(j'm'\frac{1}{2}\sigma', jm\frac{1}{2}\sigma; \hat{R})$ for the transition $(jm\frac{1}{2}\sigma) \rightarrow (j'm'\frac{1}{2}\sigma')$ by the unitary transformation[5,18]

$$f(j'm'\tfrac{1}{2}\sigma', jm\tfrac{1}{2}\sigma; \hat{R}) = \sum_{\Lambda SM_S} \langle j'm'\tfrac{1}{2}\sigma' | \Lambda SM_S\rangle \times f(\Lambda SM_S, \Lambda SM_S; \hat{R}) \langle \Lambda SM_S | jm\tfrac{1}{2}\sigma\rangle \ . \quad (13)$$

When the atomic states are also quantized with respect to the body axis $\vec{R}$, the matrix elements of this transformation are simply recoupling coefficients, viz.,

$$\langle jm\tfrac{1}{2}\sigma | \Lambda SM_S\rangle = (1m_L 00 | 1\Lambda)(1m_L \tfrac{1}{2} m_S | jm)(\tfrac{1}{2} m_S \tfrac{1}{2}\sigma | SM_S) \ . \quad (14)$$

Equation (13) provides a crude physical interpretation of the spin-change process: The C^+ and H atoms, initially in states (jm) and $(\frac{1}{2}\sigma)$, respectively, approach each other adiabatically, their angular momenta coupling to form particular CH^+ molecular stationary states $\chi(\Lambda SM_S)$; then, after scattering elastically, the atoms separate and each molecular state is "uncoupled," yielding mixtures of final atomic states $(j'm')$ and $(\frac{1}{2}\sigma')$. This interpretation suggests the following prescription for including the spin-change process in the close-coupling formalism. We begin with the coupled equations (7) and retain only those coupling terms arising from the ground-state configurations $C^+(^2P)$ and $H(^2S)$. Dropping the constant total angular momentum $j_\beta = \frac{1}{2}$ of the hydrogen atom from the notation, the coupling matrix element becomes

$$V^J_{\gamma\gamma'}(R) = \langle \Gamma^{JM}_{jl\mathcal{J}} | V | \Gamma^{JM}_{j'l'\mathcal{J}'}\rangle = \sum (jmlm_l | \mathcal{J}\mathfrak{M})(\mathcal{J}\mathfrak{M}\tfrac{1}{2}\sigma | JM)(j'm'l'm'_l | \mathcal{J}'\mathfrak{M}')(\mathcal{J}'\mathfrak{M}'\tfrac{1}{2}\sigma' | JM) \times \langle Y_{lm_l}(\hat{R})\psi_{C^+}(jm)\psi_H(\tfrac{1}{2}\sigma) | V | Y_{l'm'_l}(\hat{R})\psi_{C^+}(j'm')\psi_H(\tfrac{1}{2}\sigma')\rangle \ , \quad (15)$$

where the summation is over all projection quantum numbers except M.

Now the antisymmetrized product function $\psi_{C^+}(jm)\psi_H(\frac{1}{2}\sigma)$, quantized with respect to the incident-beam direction, is related to the antisymmetrized product function $\phi_{C^+}(j\tilde{m})\phi_H(\frac{1}{2}\tilde{\sigma})$, quantized with respect to the body axis, by the relation

$$\psi_{C^+}(jm)\psi_H(\tfrac{1}{2}\sigma) = \sum_{\tilde{m}\tilde{\sigma}} D^j_{\tilde{m}m}(\varphi_{R'}, \vartheta_{R'}, 0) D^{1/2}_{\tilde{\sigma}\sigma}(\varphi_{R'}, \vartheta_{R'}, 0) \phi_{C^+}(j\tilde{m})\phi_H(\tfrac{1}{2}\tilde{\sigma}) = \sum_{\tilde{m}\tilde{\sigma}} D^j_{\tilde{m}m}(\hat{R}) D^{1/2}_{\tilde{\sigma}\sigma}(\hat{R}) \phi_{C^+}(j\tilde{m})\phi_H(\tfrac{1}{2}\tilde{\sigma}) \ , \quad (16)$$

where the coefficients D are elements of the rotation matrices.[19] Further, the wave function $\phi_{C^+}(j\tilde{m})\phi_H(\frac{1}{2}\tilde{\sigma})$ is related asymptotically to the molecular stationary states $\chi(\Lambda SM_S)$ by the recoupling transformation (13),

$$\phi_{C^+}(j\tilde{m})\phi_H(\tfrac{1}{2}\tilde{\sigma}) \sim \sum_{\Lambda SM_S} \chi(\Lambda SM_S)\langle \Lambda SM_S | j\tilde{m}\tfrac{1}{2}\tilde{\sigma}\rangle \ . \quad (17)$$

We now assume for the sake of simplicity that this recoupling is valid at *all* internuclear separations R. On substituting (16) and (17) into (15), the integral over the configuration space of all electrons becomes

$$\langle \chi(\Lambda SM_S) | V | \chi(\Lambda SM_S)\rangle \ .$$

If we neglect at this point the $C^+(^2P)$ energy defect and spin-orbit and spin-spin terms in the interaction V, all in keeping with the spin-change formalism described above, it follows that V is diagonal in the (ΛSM_S) representation and, for a given Λ and S, is independent of M_S, and that the above matrix element may be approximated by

$$\langle \chi(\Lambda SM_S) | V | \chi(\Lambda SM_S)\rangle \equiv v_{\Lambda S}(R) = E_{\Lambda S}(R) + V_N - \langle \chi(\Lambda SM_S) | \mathcal{H}_{C^+} + \mathcal{H}_H | \chi(\Lambda SM_S)\rangle \simeq E_{\Lambda S}(R) + V_N - [E_{C^+}(^2P) + E_H(^2S)] \ . \quad (18)$$

Here, $E_{\Lambda S}(R)$ is the electronic energy of the molecular state $\chi(\Lambda SM_S)$ and V_N is the Coulomb interaction of the two nuclei. Equation (18) is correct asymptotically [for a given $C^+(^2P_j)$ level], and should be reasonably accurate at small internuclear

separations since the quantity

$$\langle \chi(\Lambda S M_S) | \mathcal{H}_C + \mathcal{H}_H | \chi(\Lambda S M_S) \rangle$$

is not strongly R dependent. For consistency we use $E_{C^+}(^2P_{1/2})$ in Eq. (18) throughout our calculations, and allow for the energy defect by using the correct k_j^2 in the scattering equations (7).

Upon combining the results Eqs. (16)–(18), substitution into Eq. (15) yields

$$\langle \Gamma^{JM}_{jl\mathcal{J}} | V | \Gamma^{JM}_{j'l'\mathcal{J}'} \rangle = \sum v_{\Lambda S}(R)(jml m_l | \mathcal{J}\mathfrak{M})$$
$$\times (\mathcal{J}\mathfrak{M}\tfrac{1}{2}\sigma | JM)(j'm'l'm_l' | \mathcal{J}'\mathfrak{M}')(\mathcal{J}'\mathfrak{M}'\tfrac{1}{2}\sigma' | JM)$$
$$\times \langle j\tilde{m}\tfrac{1}{2}\tilde{\sigma} | \Lambda S M_S \rangle \langle \Lambda S M_S | j'\tilde{m}'\tfrac{1}{2}\tilde{\sigma}' \rangle$$
$$\times \langle Y_{lm_l}(\hat{R}) D^{j}_{\tilde{m}m}(\hat{R}) D^{1/2}_{\tilde{\sigma}\sigma}(\hat{R}) | Y_{l'm_l'}(\hat{R}) D^{j'}_{\tilde{m}'m'}(\hat{R}) D^{1/2}_{\tilde{\sigma}'\sigma'}(\hat{R}) \rangle , \quad (19)$$

where the summation is over Λ and S and again over all projection quantum numbers except M. In the Appendix this expression is shown to reduce to

$$\langle \Gamma^{JM}_{jl\mathcal{J}} | V | \Gamma^{JM}_{j'l'\mathcal{J}'} \rangle = \sum_{\Lambda S} v_{\Lambda S}(R) p^J_{\Lambda S}(jl\mathcal{J}, j'l'\mathcal{J}'), \quad (20)$$

where the coupling coefficient is

$$p^J_{\Lambda S}(jl\mathcal{J}, j'l'\mathcal{J}') = (2S+1)[(2j+1)(2j'+1)(2l+1)(2l'+1)(2\mathcal{J}+1)(2\mathcal{J}'+1)]^{1/2}(-)^{-J-S-\mathcal{J}-\mathcal{J}'} \sum_{abc} (2a+1)(2b+1) \begin{pmatrix} l & l' & c \\ 0 & 0 & 0 \end{pmatrix}$$
$$\times \begin{Bmatrix} J & l & a \\ j & \frac{1}{2} & \mathcal{J} \end{Bmatrix} \begin{Bmatrix} J & l' & b \\ j' & \frac{1}{2} & \mathcal{J}' \end{Bmatrix} \begin{Bmatrix} 1 & a & S \\ \frac{1}{2} & \frac{1}{2} & j \end{Bmatrix} \begin{Bmatrix} 1 & b & S \\ \frac{1}{2} & \frac{1}{2} & j' \end{Bmatrix} \begin{Bmatrix} l' & l & c \\ a & b & J \end{Bmatrix} \begin{Bmatrix} 1 & 1 & c \\ a & b & S \end{Bmatrix} \sum_{|m_L|=\Lambda} (-)^{m_L} \begin{pmatrix} 1 & 1 & c \\ -m_L & m_L & 0 \end{pmatrix} . \quad (21)$$

Because here $S = 0$ or 1, the summation indices a and b are restricted to the values 0, 1, and 2; in addition, from the summation with respect to m_L, c is restricted to the values 0 or 2.

Thus, as the atoms approach each other along the various possible potential energy curves, the coupling terms Eqs. (20) allow for electron exchange in each molecular state $\chi(\Lambda S)$ via the angular momentum recoupling characteristic of spin-change collisions.

To incorporate both the spin-change and the long-range electrostatic coupling terms in the scattering equations in a consistent manner, we take advantage of the fact that the $v_{\Lambda S}(R)$ tend asymptotically to the common value $v_0(R)$. We note also that the spin-change coupling coefficients summed over Λ and S give [15]

$$\sum_{\Lambda S} p^J_{\Lambda S}(jl\mathcal{J}, j'l'\mathcal{J}') = \delta(j,j')\delta(l,l')\delta(\mathcal{J},\mathcal{J}')$$
$$= q_0(jl\mathcal{J}, j'l'\mathcal{J}') , \quad (22)$$

so that the spin-change coupling matrix element behaves asymptotically as

$$\langle \Gamma^{JM}_{jl\mathcal{J}} | V | \Gamma^{JM}_{j'l'\mathcal{J}'} \rangle \sim v_0(R) q_0(jl\mathcal{J}, j'l'\mathcal{J}') . \quad (23)$$

Consequently, our prescription for including both types of coupling in the scattering equations is as follows. At some intermediate value $R = R_m$, where $v_0 \gg v_2$ and where all $v_{\Lambda S}$ have approached nearly the same value, we match the $v_{\Lambda S}$ to v_0, requiring

$$v_{\Lambda S}(R) \equiv v_0(R) \quad \text{for all} \quad R \geq R_m . \quad (24)$$

From Eq. (22) we observe that there is no spin-change coupling for $R \geq R_m$. Then for $R < R_m$, v_2 is rapidly cut off, since in this inner region it is effectively contained in the $v_{\Lambda S}$. In our calculations v_2 is modified to

$$\tilde{v}_2(R) = v_2(R)(1 - e^{-(R/\rho)^n}) , \quad (25)$$

where the value $n = 16$, chosen arbitrarily, is used throughout. The sensitivity of the cross sections to different values of ρ in the range $6 \leq \rho \leq 10$ is very slight, as shown later.

Finally, using the results of Eq. (12), (20), (23), and (25) the scattering equations take the explicit form

$$\left[\frac{d^2}{dR^2} - \frac{l(l+1)}{R^2} + k_j^2\right] f^J_{jl\mathcal{J}, j_0 l_0 \mathcal{J}_0}(R)$$
$$= 2\mu \sum_{j'l'\mathcal{J}'} \left[\sum_{\Lambda S} v_{\Lambda S}(R) p^J_{\Lambda S}(jl\mathcal{J}, j'l'\mathcal{J}') + \tilde{v}_2(R) q_2(jl\mathcal{J}, j'l'\mathcal{J}')\right] f^J_{j'l'\mathcal{J}', j_0 l_0 \mathcal{J}_0}(R) . \quad (26)$$

Examination of the coupling terms in Eq. (26) reveals that for each value of J, there are 12 coupled differential equations. Fortunately each set of 12 equations separates owing to parity conservation into two smaller sets of six, one containing only even partial waves l, the other only odd partial waves. These are subsequently referred to as even and odd parity channels.

Scattering cross sections are calculated from the asymptotic form of the solutions $f^J_{\gamma\gamma_0}(R)$. At large separations R the coupling matrix elements are effectively zero and, *for each J value*, the matrix of solutions $\underline{f}^J$ has the form[20]

$$\underline{f}(R) = \underline{J}(R)\underline{A}_1 + \underline{N}(R)\underline{A}_2 \ , \tag{27}$$

where

$$J_{\mu\nu}(R) = \delta(\mu,\nu)k_\mu R j_{l_\mu}(k_\mu R) \ , \tag{28}$$

$$N_{\mu\nu}(R) = -\delta(\mu,\nu)k_\mu R n_{l_\mu}(k_\mu R) \ , \tag{29}$$

j_l and n_l are the spherical Bessel functions of the first and second kinds, and $\underline{A}_1$ and $\underline{A}_2$ are constant matrices of coefficients.

Defining a momentum matrix with elements

$$K_{\mu\nu} = \delta(\mu,\nu)k_\mu \ , \tag{30}$$

it follows that the R matrix for a specific J value is given by

$$\underline{R}^J = \underline{K}^{1/2}(\underline{A}_2\underline{A}_1^{-1})\underline{K}^{-1/2} \ . \tag{31}$$

The cross section $Q(j',j)$ for the $C^+(^2P)$ fine-structure transition $j \to j'$ may then be computed from the expression[21]

$$Q(j',j) = \frac{\pi}{k_j^2}\sum_{J=0}^{\infty}\frac{2J+1}{(2j+1)(2)}\sum_{ll'jj'}|T^J_{\gamma'\gamma}|^2 \ , \tag{32}$$

the R and T matrices being related by

$$\underline{T}^J = 2i\underline{R}^J/(1 - i\underline{R}^J) \ . \tag{33}$$

The factor of 2 in the denominator of (32) is the constant statistical weight of the ground-state hydrogen atom.

III. NUMERICAL PROCEDURES

Explicit knowledge of the potential energy curves of CH^+ states arising from the ground configurations $C^+(^2P)$ and $H(^2S)$ is required to compute the spin-change coupling matrix elements. For the $^3\Sigma^+$ and $^3\Pi$ states, we have used the data given by Moore,[9] and for the $^1\Sigma^+$ and $^1\Pi$ states, the data communicated by Browne.[10] All of these data are listed in Table I.

For our purposes, each of the four potential energy curves is appropriately increased or decreased a constant amount at all R values so that asymptotically each one has the value of the total $C^+(^2P) + H(^2S)$ separated atom energy, computed by Clementi[22] to be -37.792 a.u. Then the curves $v_{\Lambda S}$ are found simply by subtracting the separated atom energy from each potential energy curve. A Lagrangian interpolation scheme is used to obtain values of the $v_{\Lambda S}$ at each point in the numerical integration.

Now in the calculations, the CH^+ interaction potentials $v_{\Lambda S}$ are assumed to approach each other and match at some intermediate point R_m. The matching is accomplished by providing a linear fit for each adjusted potential between $R = 5a_0$ and the chosen match point $R_m > 5a_0$.

In all of our computations the value $R_m = 6a_0$ was used. The sensitivity of the cross sections to larger values of R_m is discussed in Sec. IV; however, we expect it to be small because even at $R_m = 6$ it turns out that the $^1\Sigma^+$, $^1\Pi$, and $^3\Pi$ potential energies are altered only very slightly. The altered repulsive $^3\Sigma^+$ potential energy $v(^3\Sigma^+)$ is changed from its adjusted value of 0.000 a.u. to the value -0.00216 a.u. $= v_0(6)$. Since all four interaction potentials should be attractive in the asymptotic region, such alterations are not considered unreasonable.

TABLE I. CH^+ $^3\Sigma^+$, $^3\Pi$, $^1\Sigma^+$, and $^1\Pi$ potential energy curves. Data are from Refs. 9 and 10.

$R(a_0)$	$^3\Sigma^+$(a.u.)	$^3\Pi$(a.u.)	$^1\Sigma^+$(a.u.)	$^1\Pi$(a.u.)
1.0			−37.046	−36.907
1.5			−37.767	−37.612
1.7			−37.855	−37.701
1.9	−37.284	−37.793	−37.898	−37.474
2.0	−37.337			
2.1		−37.815		
2.2	−37.427		−37.916	−37.778
2.3		−37.821	−37.916	−37.782
2.4	−37.499		−37.913	−37.785
2.5		−37.819	−37.909	−37.785
2.7	−37.580			
2.8			−37.891	−37.785
3.0	−37.636	−37.805	−37.878	−37.782
3.5	−37.692		−37.846	−37.775
4.0		−37.781	−37.823	−37.769
5.0	−37.743		−37.803	−37.760
6.0	−37.748	−37.770		
7.0			−37.797	−37.754
10.0		−37.769	−37.797	−37.753

The quantity

$$\langle r_{2p}^2\rangle = \langle\psi_{C^+}(2p)|\,r^2\,|\psi_{C^+}(2p)\rangle = 2.689a_0^2 \ , \tag{34}$$

which appears in the long-range interaction potentials $v_\lambda(R)$ of Eqs. (12), is computed from Clementi's atomic-wave-function data.[22]

The integration of the coupled equations (29) is performed numerically using the Numerov algorithm.[20,23] For this algorithm the integration is started by specifying each solution at two successive integration points. The CH^+ interaction potentials $v_{\Lambda S}$ are highly repulsive at small internuclear separations, and consequently the solutions $f^J_{\gamma\gamma_0}$ are unstable if the initial integration point is at or very near the origin. (This problem is considered in some detail by Allison and Burke.[21]) In addition, large differences may exist among the diagonal coupling terms $V^J_{\gamma\gamma}$ at small R values, resulting in significantly different classical turning points for scattering channels with small l values.

Various schemes were devised to avoid numerical difficulties, while at the same time starting the integrations as close to the origin as possible. The method settled upon consists of starting each solution $f^J_{\gamma\gamma_0}$ separately at R_γ where the diagonal term

$$U_\gamma = 2\mu V_\gamma(R_\gamma) \equiv 2\mu \left[V^J_{\gamma\gamma}(R_\gamma) + \frac{l(l+1)}{R_\gamma^2} - k_j^2 \right] \qquad (35)$$

first becomes less than some prescribed value U_0. For consistency the solutions f^J_{γ',γ_0} generated through off-diagonal coupling terms $V^J_{\gamma\gamma'}$ are reset to zero at each integration point as long as $U_{\gamma'} > U_0$. A typical value of U_0 is 50. The sensitivity of the cross sections to different values of U_0 is noted in our discussion of the results; because of the centrifugal barrier $l(l+1)/R^2$, this sensitivity should decrease with increasing l.

Having been started in this way, the numerical integration is continued into the asymptotic region, $R_{\max} \gtrsim 100$. Integration step sizes that provide a good compromise between speed and accuracy are

$$\Delta R = 0.01 \quad \text{for } R \leq 6.4 ,$$

$$\Delta R = 0.02 \quad \text{for } 6.4 < R \leq 26.4 ,$$

$$\Delta R = 0.16 \quad \text{for } 26.4 < R_{\max} .$$

These step sizes correspond to approximately $\frac{1}{20}$ of the average effective de Broglie wavelength in each region.

Next, the R matrices are found by matching the asymptotic solutions to spherical Bessel functions, as in Eq. (27). The actual procedure is discussed elsewhere.[15,20] By computing R matrices at further integration points the convergence of the solutions may be ascertained. In addition, some measure of the numerical error may be obtained by examining the asymmetry of the R matrices. In all cases, the dominant (largest in magnitude) off-diagonal R-matrix elements agree to at least 1 part in 1000.

Finally, the T matrices and then the cross sections are calculated from Eqs. (36) and (35).

IV. RESULTS AND CONCLUSIONS

The C^+-H scattering cross sections have been calculated for seven center-of-mass energies E ranging from 0.0100 to 0.0850 eV. These values and the corresponding values of $k^2 = 2\mu E$ and $T(^\circ\mathrm{K}) = E/k_B$ are given in Table II. The $C^+(^2P_{1/2})$ $\rightarrow C^+(^2P_{3/2})$ threshold is included also.

TABLE II. Center-of-mass energies for C^+-H collisions. $C^+(^2P)$ energy defect is shown as ΔE, Δk^2, and ΔT.

E (eV)	k^2	T (°K)
($\Delta E = 0.0079$)	($\Delta k^2 = 0.9961$)	($\Delta T = 92.1$)
0.0100	1.255	116.0
0.0125	1.569	145.0
0.0150	1.882	174.1
0.0175	2.196	203.1
0.0275	3.451	319.1
0.0500	6.275	580.0
0.0850	10.67	986.4

TABLE III. C^+-H total cross sections (a_0^2). (j', j) indicates the transition $C^+(^2P_j) \rightarrow C^+(^2P_{j'})$.

k^2	$(\frac{1}{2}, \frac{1}{2})$	$(\frac{1}{2}, \frac{3}{2})$	$(\frac{3}{2}, \frac{1}{2})$	$(\frac{3}{2}, \frac{3}{2})$
1.255	2478	417.2	174.0	3989
1.569	2271	268.4	196.0	3174
1.882	2138	210.2	198.4	2571
2.196	2055	165.8	181.1	2462
3.451	1623	110.5	157.0	1986
6.275	1305	68.7	115.6	1442
10.67	1177	56.5	102.4	1392

In order to reduce the amount of computation, the scattering equations were, at each energy, solved for channels of both parities but only even $J \leq 30$, denoted $J = 0(2)30$, and beyond in steps of 5, i.e., $J = 35(5)50$. Now for $J = 0$, there are just two channels with a given parity, for $J = 1$, five channels, and for $J \geq 2$, six channels. Hence, the formula we use to estimate each total cross section is

$$Q = Q(0^+) + Q(0^-) + 2 \sum_{J=2(2)30} [Q(J^+) + Q(J^-)] + 5 \sum_{J=35(5)50} [Q(J^+) + Q(J^-)] , \qquad (36)$$

where $Q(J^+)$ and $Q(J^-)$ are, respectively, the sums of the partial cross sections of even and odd parity channels having a total angular momentum J. Total cross sections at each energy, computed from Eq. (36), are presented in Table III.

To estimate the accuracy of the above procedure, the partial cross sections $Q(J)$ at $k^2 = 1.255$ were also computed for the odd values $J = 1(2)19$. We find that for the excitation process $^2P_{1/2} \rightarrow {}^2P_{3/2}$,

$$Q(\text{even } J) = \sum_{J=2(2)20} [Q(J^+) + Q(J^-)] = 88.4 a_0^2 ,$$

$$Q(\text{odd } J) = \sum_{J=1(2)19} [Q(J^+) + Q(J^-)] = 84.9 a_0^2 .$$

The difference between these two values is an indication of the error incurred by the use of Eq. (36).

Figure 1 depicts the partial cross sections $Q(J^+)$ and $Q(J^-)$ for elastic $(\frac{1}{2}, \frac{1}{2})$ scattering at $k^2 = 1.255$. The oscillatory behavior, characteristic of heavy-particle collisions, is typical of the C^+-H elastic cross sections at all energies considered.

The excitation cross section $(\frac{3}{2}, \frac{1}{2})$ at $k^2 = 1.255$ is plotted vs J in Fig. 2. The peaks and valleys in the excitation cross section in general coincide with those in the elastic cross section. This is not surprising since, at small nuclear separations, the off-diagonal coupling matrix elements $V_{\gamma\gamma'}(R)$ are frequently as large as the diagonal ones.

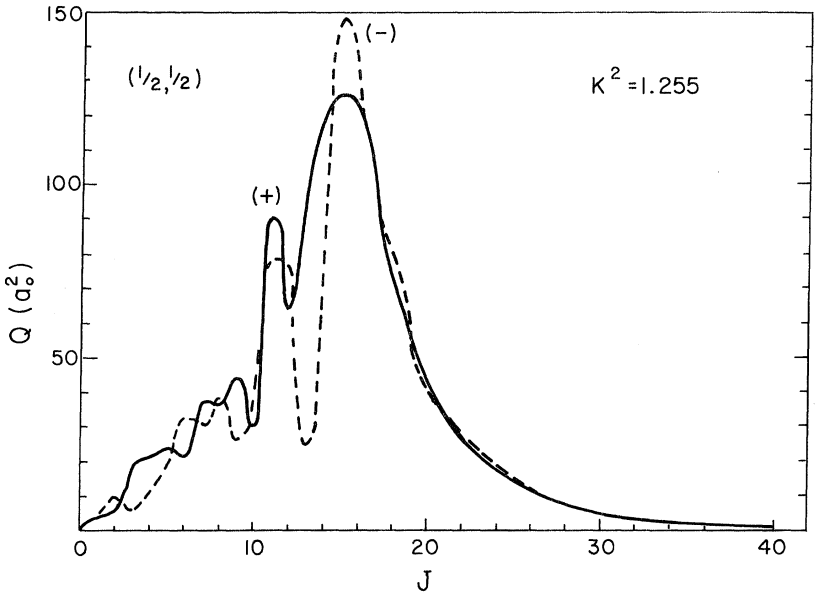

FIG. 1. Partial elastic ($\frac{1}{2}$, $\frac{1}{2}$) cross sections (a_0^2) for even (+) and odd (−) parity scattering channels plotted vs J, for the incident energy $k^2 = 1.255$.

Figure 3 shows the partial excitation cross sections at the highest energy considered, $k^2 = 10.67$. The oscillations are not so pronounced here because only even-J-value partial cross sections have been computed and plotted. Of course, the increase in k^2 allows more partial waves (higher J values) to contribute significantly to the total cross section.

A principal objective of this investigation is to determine the relative importance of the two coupling mechanisms described earlier. To this end, we repeated the calculations at $k^2 = 10.67$ for several even-parity channels, including *only* the spin-change coupling matrix elements, i.e., $\tilde{v}_2 = 0$. In Fig. 4 partial excitation cross sections obtained in this approximation (SC) are compared with those of the full calculation (LRSC), which include both long-range and spin-change coupling terms. The two coupling mechanisms interfere with each other in a complicated manner, and it is clear that in our formalism spin-change coupling is much more important. Additional tests indicate that this conclusion is correct throughout the energy range considered in our investigation. Furthermore, this observation provides an explanation of the sharp cutoff in the partial excitation cross-section distributions evident in Figs. 2 and 3. Since the spin-change mechanism vanishes beyond $R = R_m$, only those scattering channels with l's, and hence J's small enough to allow significant penetration of the centrifugal barrier can measurably contribute to the total excitation cross section.

It was noted earlier that all of our calculations were performed with $R_m = 6.0$. The interaction potentials v_{AS} obtained from the data given in Table I are very close at this point and there seems little

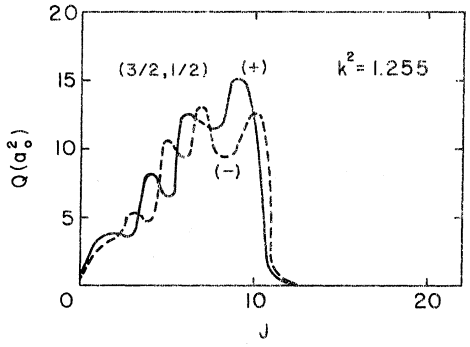

FIG. 2. Same as Fig. 1 for partial excitation ($\frac{3}{2}$, $\frac{1}{2}$) cross sections (a_0^2).

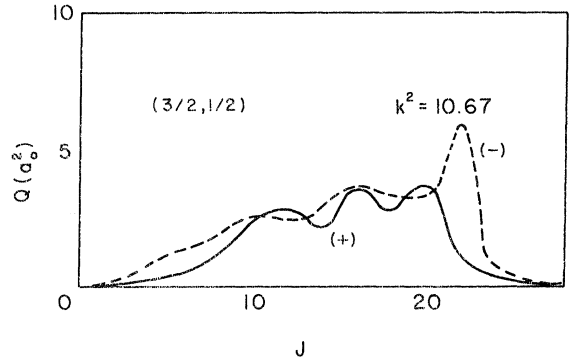

FIG. 3. Partial excitation ($\frac{3}{2}$, $\frac{1}{2}$) cross sections (a_0^2) for even (+) and odd (−) parity scattering channels plotted vs J, for the incident energy $k^2 = 10.67$. Only cross sections for even J values have been computed and plotted.

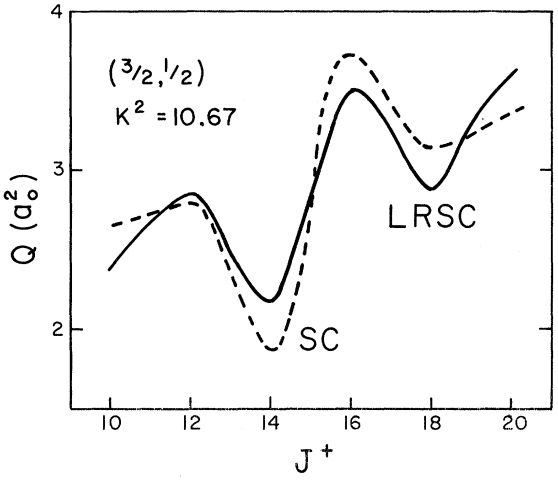

FIG. 4. Comparison of the partial excitation cross sections at $k^2 = 10.67$ computed including both long-range electrostatic and spin-change coupling terms (LRSC) with those computed including only spin-change coupling terms (SC).

justification for using a larger value of R_m. However, in light of the above comments we repeated the computations at $k^2 = 2.196$, which is near the excitation cross-section maximum, for $J^{\pm} = 0(2)22$ using the match point $R_m = 8.0$. Again, a linear fit was provided for each curve v_{AS} between $R = 5.0$ and $R = R_m$. The resulting total cross sections are $Q(\frac{1}{2},\frac{1}{2}) = 1970a_0^2$, $Q(\frac{3}{2},\frac{1}{2}) = 194.9a_0^2$, $(Q\frac{3}{2},\frac{3}{2}) = 2759a_0^2$. Comparing these values with those given in Table III we see that the differences are of the order of 10%.

We have also investigated the sensitivity of our results to the starting points for the numerical integration of the scattering equations. These points are determined by the parameter U_0 [cf. Eq. (35)]. In Table IV results obtained by using $U_0 = 50$ and $U_0 = 10$ for the case $k^2 = 1.255$, $J^+ = 1(2)9$ are given. Listed are the averages

$$\delta = \frac{1}{N}\left(\sum_{i>j}^{N}\left|1 - \frac{R_{ij}}{R_{ji}}\right|\right) , \tag{37}$$

which measure the asymmetry of the R matrix and hence the accuracy of the numerical integration, and the partial excitation cross sections. As J increases we find that smaller values of U_0 must be used to maintain good symmetry but also that the cross sections become less sensitive to the specific value of U_0 chosen. After extensive testing we chose the values $U_0 = 10$, 25, 50 for various ranges of J and k^2. The specific choices used in the calculation of the total cross sections given in Table III are $U_0 = 50$, for $J \le 8$ and all k^2, and for $J > 8$ and $k^2 > 10$; $U_0 = 25$, for $J > 8$ and $5 < k^2 \le 10$; and $U_0 = 10$, for $J > 8$ and $k^2 \le 5$. These choices yield symmetric R matrices. From data such as those given in Table IV we estimate that the error in the total cross sections due to our integration procedure is less than 5%.

We also performed three other checks on the sensitivity of our results, all involving alterations of the interaction potentials. The long-range interaction potential of Eq. (10) is based on the second-order interaction energy $\epsilon^{(2)}$ for $C^+(^2P)$ and $H(^2S)$ at large internuclear separations. The latter is given by[12]

$$\epsilon^{(2)} = \int_{\alpha\neq 0}\int_{\beta\neq 0} \frac{|\langle\psi_{C^+}(0)\psi_H(0)\,|\,V\,|\,\psi_{C^+}(\alpha)\psi_H(\beta)\rangle|^2}{[E_{C^+}(\alpha) - E_{C^+}(0)] + [E_H(\beta) - E_H(0)]} , \tag{38}$$

where the zeros represent the ground states $C^+(^2P)$ and $H(^2S)$, and the summations are over both discrete and continuum states. Equation (10) is, however, only second order in H. The resulting interaction potential is then carried only to first order in C^+ in Eq. (12) by averaging the long-range interaction v with respect to the $C^+(^2P)$ orbital. This does not result in the correct Eq. (38) because all C^+ excited states have been neglected. The energy differences in the denominator of Eq. (38) are roughly equal, suggesting that some terms in v may be too large by approximately a factor of 2. This is not true for the entire interaction potential, however, since the leading terms of $\epsilon^{(2)}$ and of v agree, both being given by $-\alpha_2/2R^4$. However, the v_2

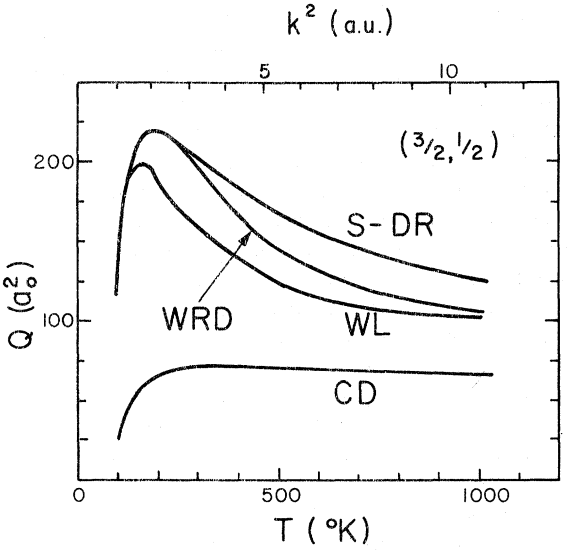

FIG. 5. Comparison of the total C^+-H excitation cross sections calculated by Smith (S-DR), Ref. 7, Callaway and Dugan (CD), Ref. 6, and Wofsy, Reid, and Dalgarno (WRD), Ref. 8, with the results of the present investigation (WL).

TABLE IV. Dependence of R-matrix symmetry and excitation cross sections with respect to U_0. $k_0^2 = 1.255$.

	$U_0 = 50$		$U_0 = 10$	
J^+	δ	$(\frac{3}{2}, \frac{1}{2})$	δ	$(\frac{3}{2}, \frac{1}{2})$
1	0.0012	3.217	0.0006	2.271
3	0.0296	3.572	0.0012	4.635
5	0.0172	6.868	0.0018	7.678
7	0.0470	11.84	0.0072	10.92
9	0.2912	14.28	0.0076	15.17

term could be too large. For this reason, the C^+-H total cross sections at $k^2 = 2.196$ were computed with $v_2 \to \frac{1}{2}v_2$. The excitation cross section changed less than 1%, and the elastic cross sections less than 5%, reaffirming our earlier conclusion that the long-range interaction v_2 does not strongly affect the scattering cross sections. In addition, varying the cutoff parameter ρ in $\tilde{v}_2$ over the range $6a_0$–$10a_0$ produced no measurable changes in the cross sections. And finally, in order to ascertain the importance of the only repulsive potential (the CH^+ $^3\Sigma^+$ state), we multiplied $v(^3\Sigma^+)$ by $\frac{1}{2}$ at all $R < 5a_0$. Total cross sections at $k^2 = 2.196$ calculated with this potential differ by less than 6% from those reported in Table III. Thus, combining these results with those of the preceding paragraphs, we estimate the C^+-H cross sections listed in Table III to be correct to within 15%, with respect to the formalism presented in Sec. II.

In Fig. 5 we compare our results (WL) for the C^+-H excitation cross section with those reported by Smith,[7] by Callaway and Dugan,[6] and by Wofsy *et al.*[8] We recall the Smith's results (S-DR) are obtained from a correction to the elastic orbiting approximation calculation by Dalgarno and Rudge,[3] and do not include the specific forms of the CH^+ potential energy curves. The results of Callaway and Dugan (CD) are obtained from an impact-parameter approximation by considering only the long-range interaction, neglecting the true elastic scatterings, and assuming the excitation collision to be elastic. The cross section reported by Wofsy *et al.* (WRD) is computed using the elastic spin-change formalism (described in detail by Smith[5]). Furthermore, Smith, Callaway and Dugan, and Wofsy *et al.* multiply their cross sections by the ratio of the final to initial relative velocities to take approximate account of the energy defect between the $C^+(^2P_j)$ levels.

Considering results such as those illustrated in Fig. 4, which indicate the importance of the spin-change process, it is quite reasonable that our calculations agree more closely with those of Wofsy *et al.* and with Smith. We investigated this possibly fortuitous agreement further by recomputing the total cross sections at $k^2 = 10.67$ with $\Delta k^2 = 0$ and $\tilde{v}_2 = 0$ to simulate the WRD calculation. In this way, we obtain $Q(\Delta k^2 = 0,\ v_2 = 0) = 96.64a_0^2$, which differs by only 6% from the value given in Table III and by only 5% from the value reported by WRD, and which is about 18% lower than that calculated by S-DR. Thus, at least at this energy, the approximations $\Delta k^2 = 0$ and $\tilde{v}_2 = 0$ have only a slight effect on the results of the close-coupling calculations. At lower energies, of course, the approximation $\Delta k^2 = 0$ is expected to be worse.

In addition to the above-mentioned investigations, total cross sections were calculated at $k^2 = 10.67$ with the spin-change coupling terms omitted. The spherical potential v_0 was transformed at small R to an admixture of CH^+ interaction potentials, as in our full calculations. The resulting excitation cross section, Q (no spin-change coupling) $= 3.13a_0^2$, is more than an order of magnitude smaller than the value given by CD. It is difficult to give specific reasons for this large discrepancy, but one point in particular should be made. In their impact-parameter formulation CD only considered the nonspherical interaction potential v_2. The spherical term v_0, which does not couple the $C^+(^2P)$ fine-structure levels, but which largely determines the trajectories of the atoms at large internuclear separations, is neglected.

We conclude our presentation of results with a brief discussion of the rate of cooling of interstellar matter due to the radiative deexcitation of $C^+(^2P_{3/2})$. A polynomial fit to the total C^+-H excitation cross section was obtained and the cooling-rate coefficient

$$\lambda_{C^+}(\tfrac{1}{2}, \tfrac{3}{2}) = \Delta E \int_{u_0}^{\infty} du\,[u f(u, T) Q_{3/2,1/2}(u)] \qquad (39)$$

calculated at several temperatures. Here, $u_0 = (2\Delta E/\mu)^{1/2}$, and $f(u, T)$ is the Maxwellian velocity distribution function for the gas at a temperature T. These rate coefficients are listed in Table V together with the total cooling-rate coefficients

$$\lambda_0 = \lambda_0(2, 0) + \lambda_0(2, 1) \qquad (40)$$

for $O(^3P_2) + H$ excitation collisions calculated by WRD.[8]

Since the two rate coefficients are roughly com-

TABLE V. Cooling-rate coefficients λ (erg cm^3 sec^{-1}) for the radiative deexcitation of C^+ $(^2P_{3/2})$ and $O(^3P) = O(^3P_1) + O(^3P_0)$ after C^+-H and O-H excitation collisions. (Oxygen data are from Ref. 8.)

T (°K)	$10^{24}\lambda_{C^+}$	$10^{24}\lambda_0$
100	6.53	0.898
125	7.73	1.50
150	8.74	2.16
200	10.1	3.45
300	11.7	5.84
500	13.8	9.62

parable, the relative importance of the two fine-structure cooling mechanisms in a given situation depends upon the relative abundances of neutral oxygen and ionized carbon.

It is unfortunate that there are no experimental results with which to compare the calculated cross sections. The lack of data for this and other similar fine-structure excitation processes in atom-atom collisions, however, emphasizes the need for precise theoretical calculations.

There are various ways in which the calculations we have reported may be improved. It would be desirable to ascertain what effect a transformation similar to Eq. (17) but R dependent would have on the results. It would also be preferable to devise a better method for starting the numerical intergrations. We hope to include these improvements in future investigations.

ACKNOWLEDGMENTS

The authors wish to thank Professor Alex Dalgarno for enlightening discussions and Professor Jim Browne for providing unpublished calculations of CH^+ potential energy curves. One of us (J.C.W.) would also like to express his appreciation to the Research Computation Center and the Chemistry Department of the University of Texas (Austin) for their hospitality during his frequent visits.

APPENDIX

In this section the spin-change coupling coefficients $p^J_{\Lambda S}(jl\mathcal{J},j'l'\mathcal{J}')$ are reduced. From Eqs. (19) and (20) we have

$$p^J_{\Lambda S}(jl\mathcal{J},j'l'\mathcal{J}')=\sum (jml m_l|\mathcal{J}\mathfrak{M})(\mathcal{J}\mathfrak{M}\tfrac{1}{2}\sigma|JM)(j'm'l'm_l'|\mathcal{J}'\mathfrak{M}')(\mathcal{J}'\mathfrak{M}'\tfrac{1}{2}\sigma'|JM)\langle j\tilde{m}\tfrac{1}{2}\tilde{\sigma}|\Lambda SM_S\rangle\langle\Lambda SM_S|j'\tilde{m}'\tfrac{1}{2}\tilde{\sigma}'\rangle$$
$$\times\langle Y_{lm_l}(\hat{R})D^{j}_{\tilde{m}m}(\hat{R})D^{1/2}_{\tilde{\sigma}\sigma}(\hat{R})|\,Y_{l'm_l'}(\hat{R})D^{j'}_{\tilde{m}'m'}(\hat{R})D^{1/2}_{\tilde{\sigma}'\sigma'}(\hat{R})\rangle\ , \tag{A1}$$

where the summation is to be performed over all projection quantum numbers $\mathfrak{M}\mathfrak{M}'m_lm_l'mm'\sigma\sigma'\tilde{m}\tilde{m}'\tilde{\sigma}\tilde{\sigma}'M_S$.

Evaluating first the integral over $\hat{R}$, we make use of the following relationships[19]:

$$Y_{\lambda\mu}(\hat{R})=\left(\frac{2\lambda+1}{4\pi}\right)^{1/2}D^{*\lambda}_{\mu 0}(\hat{R})\ , \tag{A2}$$

$$D^{\lambda}_{\mu m}(\hat{R})D^{\lambda'}_{\mu' m'}(\hat{R})=\sum_{l\nu n}(2l+1)\begin{pmatrix}\lambda & \lambda' & l\\ \mu & \mu' & \nu\end{pmatrix}\begin{pmatrix}\lambda & \lambda' & l\\ m & m' & n\end{pmatrix}D^{*l}_{\nu n}(\hat{R})\ , \tag{A3}$$

and

$$\int d\hat{R}\,D^{\lambda_1}_{\mu_1 m_1}(\hat{R})D^{\lambda_2}_{\mu_2 m_2}(\hat{R})D^{\lambda_3}_{\mu_3 m_3}(\hat{R})=4\pi\begin{pmatrix}\lambda_1 & \lambda_2 & \lambda_3\\ \mu_1 & \mu_2 & \mu_3\end{pmatrix}\begin{pmatrix}\lambda_1 & \lambda_2 & \lambda_3\\ m_1 & m_2 & m_3\end{pmatrix}\ . \tag{A4}$$

Substituting Eq. (A2) and using Eq. (A3) three times we obtain

$$\langle Y_{lm_l}D^{j}_{\tilde{m}m}D^{1/2}_{\tilde{\sigma}\sigma}|\,Y_{l'm_l'}D^{j'}_{\tilde{m}'m'}D^{1/2}_{\tilde{\sigma}'\sigma'}\rangle=(-)^{m_l}(2l+1)^{1/2}(2l'+1)^{1/2}\sum(2a+1)(2b+1)(2c+1)(-)^{\tilde{\beta}-\beta}$$
$$\times\begin{pmatrix}l & l' & c\\ 0 & 0 & 0\end{pmatrix}\begin{pmatrix}l & l' & c\\ -m_l & m_l' & \tilde{\gamma}\end{pmatrix}\begin{pmatrix}j & \frac{1}{2} & a\\ \tilde{m} & \tilde{\sigma} & \tilde{\alpha}\end{pmatrix}\begin{pmatrix}j & \frac{1}{2} & a\\ m & \sigma & \alpha\end{pmatrix}\begin{pmatrix}j' & \frac{1}{2} & b\\ \tilde{m}' & \tilde{\sigma}' & \tilde{\beta}\end{pmatrix}\begin{pmatrix}j' & \frac{1}{2} & b\\ m' & \sigma' & \beta\end{pmatrix}\begin{pmatrix}a & b & c\\ \tilde{\alpha} & -\tilde{\beta} & \tilde{\gamma}\end{pmatrix}\begin{pmatrix}a & b & c\\ \alpha & -\beta & 0\end{pmatrix}\ , \tag{A5}$$

the summation being with respect to $a\alpha\tilde{\alpha}b\beta\tilde{\beta}c\gamma$.

Now substituting Eqs. (A5) and (14) into Eq. (A1) and using 3-j symbols throughout, we employ the identities

$$\begin{pmatrix}j_1 & j_2 & j_3\\ m_1 & m_2 & m_3\end{pmatrix}\begin{Bmatrix}j_1 & j_2 & j_3\\ l_1 & l_2 & l_3\end{Bmatrix}=\sum_{n_1n_2n_3}(-)^{l_1+l_2+l_3+n_1+n_2+n_3}\begin{pmatrix}j_1 & l_2 & l_3\\ m_1 & n_2 & -n_3\end{pmatrix}\begin{pmatrix}l_1 & j_2 & l_3\\ -n_1 & m_2 & n_3\end{pmatrix}\begin{pmatrix}l_1 & l_2 & j_3\\ n_1 & -n_2 & m_3\end{pmatrix}\ , \tag{A6}$$

$$\sum_{m_1m_2}\begin{pmatrix}j_1 & j_2 & j_3\\ m_1 & m_2 & m_3\end{pmatrix}\begin{pmatrix}j_1 & j_2 & j_3'\\ m_1 & m_2 & m_3'\end{pmatrix}=\frac{\delta(j_3,j_3')\delta(m_3,m_3')}{2j_3+1}\ , \tag{A7}$$

to sum first over $m'\sigma'\mathfrak{M}'$ and $m\sigma\mathfrak{M}$, then over $\tilde{m}'\tilde{\sigma}'m_S'$ and $\tilde{m}\tilde{\sigma}m_S$, then over $M_S\tilde{\alpha}\tilde{\beta}$ and $M\alpha\beta$, dividing by $2J+1$, and finally over m_lm_l', yielding the desired result, Eq. (21).

†Research supported in part by the U. S. Atomic Energy Commission and the National Science Foundation.

*Present address: Harvard College Observatory, Cambridge, Mass.

‡Alfred P. Sloan Fellow.

[1]N. H. Deiter and W. M. Goss, Rev. Mod. Phys. 38, 256 (1966).

[2]A. Dalgarno, Rev. Mod. Phys. 39, 850 (1967).

[3]A. Dalgarno and M. R. H. Rudge, Astrophys. J. 140, 800 (1964).

[4]J. Callaway and E. Bauer, Phys. Rev. 140, A1072 (1965).

[5]F. J. Smith, Planetary Space Sci. 14, 937 (1966).

[6]J. Callaway and A. F. Dugan, Phys. Rev. 163, 162 (1967).

[7]F. J. Smith, Monthly Notices Roy. Astron. Soc. 140, 341 (1968).

[8]S. Wofsy, R. H. G. Reid, and A. Dalgarno (unpublished).

[9]P. Moore, Ph. D. thesis [University of Texas (Austin), 1965] (unpublished).

[10]J. C. Browne (private communication).

[11]N. F. Mott and H. S. W. Massey, *The Theory of Atomic Collisions*, 3rd ed. (Oxford U. P., London, 1965).

[12]A. Dalgarno and W. D. Davison, *Advances in Atomic and Molecular Physics* (Academic, New York, 1966), Vol. 2.

[13]L. Castellejo, J. C. Percival, and M. J. Seaton, Proc. Roy. Soc. (London) A254, 259 (1960).

[14]A. Dalgarno, G. W. F. Drake, and G. A. Victor, Phys. Rev. 176, 194 (1968).

[15]J. C. Weishelt, Ph. D. thesis (Rice University, 1970) (unpublished).

[16]A. M. Arthurs and A. Dalgarno, Proc. Roy. Soc. (London) A256, 540 (1960).

[17]A. Dalgarno, Proc. Roy. Soc. (London) A262, 132 (1961).

[18]A. Dalgarno and M. R. H. Rudge, Proc. Roy. Soc. (London) A286, 519 (1965).

[19]M. E. Rose, *Elementary Theory of Angular Momentum* (Wiley, New York, 1957), Chap. IV.

[20]N. F. Lane and S. Geltman, Phys. Rev. 160, 53 (1967).

[21]D. C. S. Allison and P. G. Burke, J. Phys. B 2, 941 (1969).

[22]E. Clementi, IBM J. Res. Develop. Suppl. 9 (1965).

[23]D. R. Hartree, *The Calculation of Atomic Structures* (Wiley, New York, 1957).

PHYSICAL REVIEW A VOLUME 4, NUMBER 1 JULY 1971

Electron Impact Excitation of the Rare Gases*

P. S. Ganas† and A. E. S. Green
University of Florida, Gainesville, Florida 32601

(Received 11 January 1971)

We utilize the analytic atomic independent-particle model (IPM) of Green, Sellin, and Zachor as a basis for calculating generalized oscillator strengths for the single-particle excitations of Ne, Ar, Kr, and Xe. First, we establish averages of the experimental energy levels to arrive at single-particle states. We then adjust the two parameters so that the IPM potentials accurately characterize these excited-state energies. Using the wave functions associated with these potentials and the Born approximation, we calculate the generalized oscillator strengths for excitations to p^5ns states. A very complex nodal structure is apparent at large values of momentum transfer and a rapid decline in magnitude occurs after the second node. We may accurately characterize the results up to the second node with a convenient analytic form which leads to analytic total excitation cross sections. We use available optical oscillator strengths to normalize our results. The systematics and regularities of the parameters for various Rydberg series are discussed and approximate scaling laws are given.

I. INTRODUCTION

In a series of studies,[1–5] simple two-parameter analytic independent-particle-model (IPM) potential has been found to provide a good representation of electron-atom interactions. The data used in adjusting these two parameters have been determined by experiment[6] or by using the results of Hartree-Fock[7] (HF) or Hartree-Fock-Slater[8] (HFS) descriptions of the atom. In this work we explore further consequences of this simple realistic model by carrying out calculation of inelastic excitation cross sections for rare-gas atoms, giving particular concentration to systematic properties which are needed for applied problems.

We deal primarily with the rare gases Ne, Ar, Kr, and Xe despite the fact that there is a scarcity of experimental data with which to test our results or to readjust our parameters in the potential. However, our work is approximately consistent with the available experiment and the attempts to utilize the few available HF excited-state wave functions. It is hoped, therefore, that this work, which covers a greater number of cases and a far more extended range of momentum transfer, might provide a guideline which will stimulate further measurements on rare-gas excitation cross sections and more rigorous calculations. These are needed not